CrystEngComm

Accepted Manuscript

ROYAL SOCIETY OF CHEMISTRY

www.rsc.org/crystengcomm

Journal Name

ARTICLE

Excitation wavelength-induced color tunable and white-light emissions in lanthanide(III) coordination polymers constructed by an environment-dependent luminescent tetrazolate-dicarboxylate ligand

Received 00th January 20xx,
Accepted 00th January 20xx

DOI: 10.1039/x0xx00000x

www.rsc.org/

Yu Xiao,[a,b] Shuai-Hua Wang,[a] Fa-Kun Zheng,[*,a] Mei-Feng Wu,[c] Ju-Xu,[a] Zhi-Fa Liu,[a] Jun Chen,[a,b] Rong Li[a,b] and Guo-Cong Guo[a]

An alternative approach is demonstrated to fabricate color tunable and white-light-emitting lanthanide(III) coordination polymers (Ln-CPs) by employing a selective light-emitting tetrazolate-dicarboxylate ligand, which displays different color emissions when coordinated to different lanthanide(III) ions. The emission colour of the obtained Ln-CPs can be modulated from orange to white by simply adjusting excitation wavelengths. White-light emissions, with high color rendering index and favorable correlated color temperature, have been successfully realized in new 2D single-component Sm(III) and two-component Eu(III)-doped Gd(III) coordination polymers excited at specific excitation wavelengths.

Introduction

The optical materials exhibiting widely and continuously color tunable and white-light emissions have attracted immense interest due to their promising applications as solid-state lighting, display, biological sensing and labelling, as well as photoelectronic devices.[1] Many studies have been conducted on semiconductor quantum dots[2] and inorganic lanthanide-doped compounds,[3] or organic molecules[4] to get color tunable and white-light illuminant materials. In contrast to these materials, in recent years, lanthanide(III) coordination polymers (LnCPs), which possess rich luminous building blocks from both metal ions and organic ligands, exhibit promising advantages for simple syntheses and versatile emissions.[5] In general, color tunable and white emissions can be achieved through changing the relative amount of different light emitters,[6-8] such as incorporation different amounts of Eu(III) and Tb(III) ions to the host frameworks,[6] or encapsulation of different contents of organic fluorescent dyes within the pores of CPs,[7] as well as codoping various concentrations of multiple lanthanide(III) ions into the isostructural frameworks.[8]

In addition to the three methods mentioned above, another promising strategy is based on the variation of excitation wavelengths for modulating different chromophore emissions to achieve color tunable and white-light emissions.[9-11] For example, optimal white-light emission was achieved by shifting the excitation wavelengths in the Eu(III)-doped In(III) or Gd(III) framework[9], tunable luminescence from yellow to white was realized through varying excitation wavelengths in the Eu(III)- and Tb(III)-codoped La–Zn or Gd(III) frameworks[10], and tunable yellow-to-blue photoluminescence was acquired upon changing excitation wavelengths in Dy(III) metal–organic frameworks[11]. However, exploring LnCPs which display full-color-tunable luminescence including three primary colors (RGB) and white-light emission by varying excitation wavelengths is still a challenging task.

To obtain effective color tunable and white-light emitting materials, choosing a suitable ligand and optimizing the luminescence process are necessary.[12] Tetrazole and their derivatives are an efficient chromophores for the sensitization of Ln(III) luminescence, owing to their rigidity and aromaticity.[13] We have previously developed a class of transition metal and main group metal CPs based on tetrazolate ligands, featuring peculiar and interesting luminescent behaviours.[14] In this study we selected a tetrazolate-dicarboxylate ligand 5-(4-(tetrazol-5-yl)phenoxy)

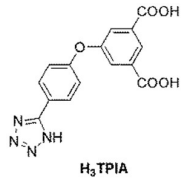

H_3TPIA

Chart 1 The chemical structure of H_3TPIA

[a] State Key Laboratory of Structural Chemistry, Fujian Institute of Research on the Structure of Matter, Chinese Academy of Sciences, Fujian, Fuzhou, 350002, PR China. E-mail: zfk@fjirsm.ac.cn; Fax: +86 591 8371 4946; Tel: +86 591 83704827
[b] University of Chinese Academy of Sciences, Beijing 100039, PR China
[c] School of Environmental and Chemical Engineering, Nanchang Hangkong University, Nanchang, Jiangxi 330063, P. R. China

† Electronic Supplementary Information (ESI) available: Additional structural tables, PXRD patterns, TGA and luminescent decay curves, UV-Vis absorption spectra and excitation spectra. CCDC 1055382, 1055383 and 1055384. For ESI and crystallographic data in CIF or other electronic format see DOI: 10.1039/x0xx00000x

isophthalic acid (H_3TPIA, Chart 1) to assemble illuminant LnCPs. As a result, a new family of isostructural LnCPs, $[Ln(TPIA)(H_2O)_3]\cdot 5.5H_2O$ (Ln = Sm **1**, Eu **2**, Gd **3**) were obtained under hydrothermal conditions. The ligand H_3TPIA shows environment-dependent selective light-emitting character with the blue fluorescence in the Sm(III) framework **1** and the dominant green phosphorescence in the Gd(III) network **3**. In the case of **1**, orange to blue tunable emissions can be achieved through modulating the intensity ratio of the blue emission of ligand and red-green emission of Sm(III) ion by varying excitation wavelengths. White-light emissions in **1** have been achieved with good color quality (Commission International de l'Eclairage (CIE) coordinate (0.33, 0.31), color-rendering index (CRI) value of 87 and correlated color temperature (CCT) value of 5748 K) excited at 358 nm. In addition, we have successfully designed and constructed a novel mixed-lanthanide CPs, $[(Eu_{0.12}Gd_{0.88})(TPIA)(H_2O)_3]\cdot 5.5H_2O$ (**4**) by doping Eu(III) ions into the Gd(III) network **3**, which exhibits an ideal white-light emission with the CIE coordinate of (0.33, 0.33), CRI value of 89, CCT magnitude of 5489 K excited at 360 nm by mixing the blue-green emission of ligand and red emission of Eu(III) ion.

Experimental section

Materials and instruments

All the chemicals were purchased commercially and used without further purification. The elemental analyses of C, H and N were performed on an Elementar Vario EL III microanalyzer. The FT-IR spectra were obtained on a VERTEX70 spectrophotometer using KBr disks in the range 4000–400 cm^{-1}. ^{1}H NMR (400 MHz) and ^{13}C NMR (101 MHz) spectra were recorded on a Bruker AVANCE 400 NMR spectrometer with Me_4Si as the internal standard in deuterated solvent DMSO-d_6. ESI mass spectra were recorded on a DECAX-30000 LCQ Deca XP mass spectrometer. Powdered X-ray diffraction (PXRD) was performed on a Rigaku MiniFlex 600 diffractometer using Cu Kα radiation (λ = 1.5406 Å) in the range of 5–50° at room temperature. Simulated PXRD patterns were derived from the Mercury Version 1.4 software (http://www.ccdc.cam.ac.uk/products/mercury/). Inductively coupled plasma spectroscopy (ICP) was performed on an Ultima 2 spectrometer. UV–visible (UV–vis) spectra were recorded at room temperature on a PerkinElmer Lambda 950 UV/vis/NIR spectrophotometer equipped with an integrating sphere in the wavelength range of 200–1200 nm. The photoluminescence (PL) and lifetime determination were conducted on a single-grating Edinburgh FL920 fluorescence spectrometer equipped with a 450 W Xe lamp, an nF900 lamp and a PMT detector. The quantum yield was measured on an Edinburgh FLS920 fluorescence spectrometer equipped with a $BaSO_4$-coated integrating sphere, a 450W Xe lamp, and a R928P PMT detector in the single-photon counting mode. The CIE coordinates, CRI and CCT were calculated using the CIE calculator-version 3 software.

Synthesis of compounds

5-(4-(tetrazol-5-yl)phenoxy) isophthalic acid (H_3TPIA). The ligand H_3TPIA can also be synthesized according to the literature method.[15,18a] The synthetic route is shown in Scheme S1. The yield of the product was 78% (based on dimethyl 5-hydroxyisophthalate). ESI–MS: m/z $[M - H]^-$, 325.4 (calcd for $C_{15}H_{10}N_4O_5$, 326.3) (Fig. S1). ^{1}H NMR (400 MHz, DMSO-d_6): δ (ppm): 8.26 (t, J = 1.4 Hz, 1H), 8.08 (d, J = 8.8 Hz, 2H), 7.74 (d, J = 1.5 Hz, 2H), 7.30 (d, J = 8.8 Hz, 2H) (Fig. S2). ^{13}C NMR (101 MHz, DMSO-d_6): δ (ppm): 166.33, 158.57, 156.84, 133.76, 129.67, 125.76, 123.61, 120.22 (Fig. S3). Anal. calcd for $C_{15}H_{10}N_4O_5$: C, 55.22; H, 3.09; N, 17.17%. Found: C, 55.15; H, 2.96; N, 17.05%. Selected IR (KBr pellet, cm^{-1}): 3435 b, 2956 b, 1703 vs, 1593 m, 1500 m, 1421 m, 1260 s, 1175 m, 1071 w, 973 w, 856 w, 762 w, 684 w (Fig. S4).

$[Sm(TPIA)(H_2O)_3]\cdot 5.5H_2O$ (1). A mixture of $Sm(NO_3)_3\cdot 6H_2O$ (0.2 mmol), H_3TPIA (0.2 mmol), H_2O (8 mL) and an aqueous solution of NaOH (1 mol/L, 0.60 mL) was sealed in a poly(tetrafluoroethylene)-lined stainless steel container under autogenous pressure and then heated to 150 °C for 4 days, and cooled to room temperature at a rate of 2.5 °C/h. Platelet crystals suitable for X-ray analysis were obtained. Yield: 85% (based on Sm) for **1**, Anal. calcd for $C_{15}H_{24}N_4O_{13.5}Sm$: C, 28.72; H, 3.83; N, 8.94%. Found: C, 28.77; H, 3.84; N, 8.85%. Selected IR (KBr pellet, cm^{-1}): 3442 b, 1617 m, 1580 w, 1523 s, 1448 s, 1380 vs, 1254 s, 1208 s, 1174 m, 1113 w, 982 m, 838 w, 780 m, 718 w, 561 w (Fig. S4).

$[Eu(TPIA)(H_2O)_3]\cdot 5.5H_2O$ (2). The synthetic procedure for **2** was the same as that for **1** except that $Sm(NO_3)_3\cdot 6H_2O$ was replaced by $Eu(NO_3)_3\cdot 6H_2O$. Platelet crystals suitable for X-ray analysis were obtained. Yield: 80% (based on Eu) for **2**, Anal. calcd for $C_{15}H_{24}N_4O_{13.5}Eu$: C, 28.65; H, 3.82; N, 8.91%. Found: C, 28.80; H, 3.90; N, 8.89%. Selected IR (KBr pellet, cm^{-1}): 3444 b, 1616 m, 1580 w, 1524 s, 1450 s, 1380 vs, 1256 s, 1209 s, 1173 m, 1113 w, 983 m, 838 w, 781 m, 718 w, 563 w (Fig. S4).

$[Gd(TPIA)(H_2O)_3]\cdot 5.5H_2O$ (3). The synthetic procedure for **3** was the same as that for **1** with $Gd(NO_3)_3\cdot 6H_2O$ in place of $Sm(NO_3)_3\cdot 6H_2O$. Platelet crystals suitable for X-ray analysis were obtained. Yield: 80% (based on Gd) for **3**, Anal. calcd for $C_{15}H_{24}N_4O_{13.5}Gd$: C, 28.41; H, 3.79; N, 8.84%. Found: C, 28.56; H, 3.80; N, 8.83%. Selected IR (KBr pellet, cm^{-1}): 3445 b, 1617 m, 1583 w, 1525 s, 1449 s, 1380 vs, 1257 s, 1208 s, 1174 m, 1114 w, 983 m, 838 w, 781 m, 719 w, 564 w (Fig. S4).

$[(Eu_{0.12}Gd_{0.88})(TPIA)(H_2O)_3]\cdot 5.5H_2O$ (4) A similar process was employed to prepare **4** by adding a certain amount of $Eu(NO_3)_3\cdot 6H_2O$ and $Gd(NO_3)_3\cdot 6H_2O$ and keep the total molar amounts of Eu(III) and Gd(III) ion the same as that for **3**. Anal. calcd for $C_{15}H_{24}N_4O_{13.5}Gd_{0.88}Eu_{0.12}$: C, 28.46; H, 3.82; N, 8.85%. Found: C, 28.64; H, 3.85; N, 8.83%. Besides, a series of Eu(III)-doped frameworks with different concentrations of Eu(III) ions have been achieved. The lanthanide(III) ion content for the doped complex was obtained by inductively coupled plasma spectroscopy (ICP) (0.9, 2, 4, 6, 7, 11, 12%).

Crystal structure determination

Single-crystal X-ray diffraction measurements were performed on a Rigaku Saturn724 CCD for **1**, a Rigaku Mercury CCD for **2**,

Journal Name

ARTICLE

Table 1 Crystal data and structural refinements for compounds **1–4**

Complex	**1**	**2**	**3**	**4**
Empirical formula	$C_{15}H_{24}N_4O_{13.5}Sm$	$C_{15}H_{24}N_4O_{13.5}Eu$	$C_{15}H_{24}N_4O_{13.5}Gd$	$C_{15}H_{24}N_4O_{13.5}Gd_{0.88}Eu_{0.12}$
M_r (g mol^{-1})	626.73	628.34	633.63	633.00
Crystal system	Triclinic	Triclinic	Triclinic	Triclinic
Space group	$P\bar{1}$	$P\bar{1}$	$P\bar{1}$	$P\bar{1}$
a (Å)	9.1586(7)	9.1406(9)	9.0892(4)	9.117(2)
b (Å)	9.5032(7)	9.4909(10)	9.4506(6)	9.474(2)
c (Å)	13.9208(8)	13.9426(12)	13.9220(7)	13.956(3)
α (°)	95.383(3)	95.290(4)	95.202(4)	95.423(5)
β (°)	91.851(2)	91.860(4)	91.845(4)	91.643(4)
γ (°)	107.700(4)	107.708(4)	107.559(4)	107.538(5)
V (Å^3)	1146.80(14)	1145.00(19)	1133.23(10)	1142.2(4)
Z	2	2	2	2
D_c/ g·cm^{-3}	1.815	1.823	1.857	1.841
μ/ mm^{-1}	2.634	2.813	3.001	2.959
F(000)	624	626	628	628
Reflections collected	9546	8815	7732	16675
Unique Reflections	4267	4213	4223	4246
GOF	1.001	1.057	1.003	1.044
R_1[a] [$I > 2\sigma(I)$]	0.0307	0.0380	0.0338	0.0216
wR_2[b] (all data)	0.0747	0.1033	0.0853	0.0619
CCDC No.	1055382	1055383	1055384	1439407

[a] $R_1 = \sum(F_o - F_c)/\sum F_o$; [b] $wR_2 = [\sum w(F_o^2 - F_c^2)^2/\sum w(F_o^2)^2]^{1/2}$

XCalibur E CCD diffractometer for **3** and Rigaku Pilatus 200K CCD for **4** respectively, which were all equipped with Mo Kα radiation (λ = 0.71073 Å), using the ω-scan technique for collection of the intensity data sets. The primitive structures were solved by the direct methods and reduced by CrystalClear software.[16] Subsequent successive difference Fourier syntheses yielded the other non-hydrogen atoms. Hydrogen atoms of ligands were added geometrically and refined using the riding model. Hydrogen atoms of coordinated water molecules were located in the idealized positions and refined with the O−H distance restrained to a target value of 0.85 Å, the H···H distance to 1.34 Å and U_{iso}(H) = 1.5U_{eq}(O). However, hydrogen atoms of lattice water molecules have not been added. Final structures were refined using a full-matrix least-squares refinement on F^2. All of the calculations were performed by the Siemens SHELXTL version 5 package of crystallographic software.[17] Pertinent crystal data and structural refinement results and selected bond distances and angles for **1**, **2, 3** and **4** are listed in Tables 1 and S1, respectively.

Results and discussion

Crystal structure and characterization

Compounds **1–4** are all isostructural and crystallize in the triclinic *P*-1 space group, identified by single-crystal XRD techniques and powdered XRD patterns (Fig. S5). Uniform distribution of mixed Ln^{3+} ions with isomorphous replacement in a single phase in the bimetallic compound **4** was unequivocally manifested by electron microscopy (Fig. S6) and crystal structure data analysis (Fig. S7). The TGA diagrams of **1**, **2** and **3** are similar (Fig. S8), which show their weight loss of 24.8, 24.7 and 24.4% in the temperature range of 30–275°C, corresponding to the loss of lattice and coordinated water molecules (calcd: 24.4, 24.3 and 24.1%, respectively). Continuous heating led to the breakdown of the framework. The TGA diagram of **4** is almost coincident with the ones of **1**, **2**, **3** (Fig. S8), which indicates that **4** has similar thermal stability to **1**, **2** and **3**.

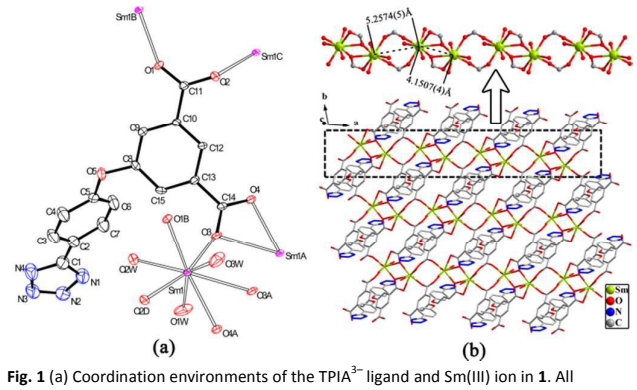

Fig. 1 (a) Coordination environments of the $TPIA^{3-}$ ligand and Sm(III) ion in **1**. All hydrogen atoms and lattice water molecules have been omitted for clarity. Symmetry codes: (A) –x, 1 – y, –z; (B) 1 – x, 2 – y, –z; (C) x, 1 + y, z; (D) x, –1 + y, z; (b) 1D zigzag chained structure along the *a* axis and the 2D network parallel to the *ab* plane.

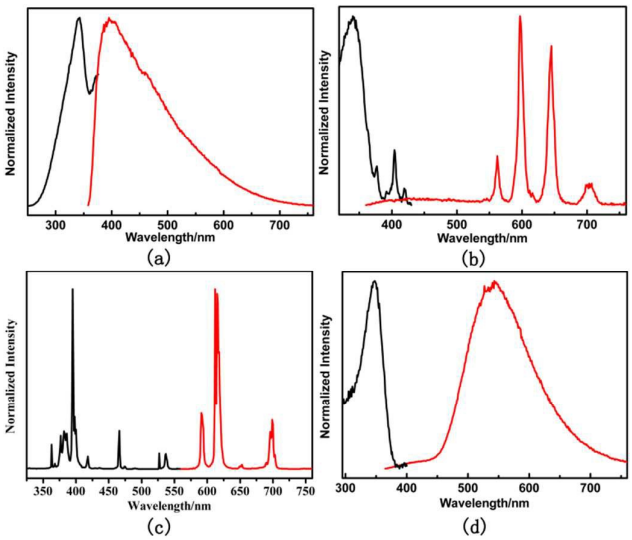

Fig. 2 The excitation (black line) and emission (red line) spectra of free ligand H_3TPIA (a), **1-Sm** (b), **2-Eu** (c) and **3-Gd** (d) at 298K, respectively.

The structure detail of **1** is outlined here as a representative example. The asymmetry unit of **1** consists of one crystallographically unique Sm(III) ion, one $TPIA^{3-}$ ligand, three coordinated water molecules and five and a half lattice water molecules. The Sm(III) ion is eight-coordinated by five carboxylate oxygen atoms from four $TPIA^{3-}$ ligands, and three coordinated water molecules, forming a distorted dodecahedron geometry (Fig. 1a). The Sm–O bond lengths are in the normal range, varying from 2.344(2) to 2.612(2) Å. The adjacent Sm(III) atoms are linked alternately by carboxylate group in two different coordination modes (bidentate bridging and chelate-bridging) with the intermetallic distances of 4.1507(4) and 5.2574(5) Å, respectively, resulting in 1D zigzag metal-carboxylato chains along the a axis. These 1D chains are further connected through $TPIA^{3-}$ ligands to form a 2D network parallel to the *ab* plane (Fig. 1b). The tetrazolate group in $TPIA^{3-}$ ligand does not participate in metal coordination.

Photoluminescence properties

Solid-state photoluminescence property of free ligand H_3TPIA, lanthanide nitrate and compounds **1–3** at room temperature was investigated. The emission spectrum of the free ligand H_3TPIA displays a wide band centered at 396 nm presumably due to $\pi^* \rightarrow \pi$ or $\pi^* \rightarrow n$ transitions under 340 nm UV light excitation (Fig. 2a).[18] Upon excitation at 340 nm, compound **1** displays multiple emission peaks at 460, 562, 597, 645 and 706 nm (Fig. 2b). The broad band centered at 460 nm is apparently reminiscent of the emission from the ligand center, while the four other narrow peaks originate from the $^4G_{5/2}$-^6H_J (J = 5/2, 7/2, 9/2, 11/2) transitions of Sm(III) ion.[19] The luminescence lifetime (τ) value for the $^4G_{5/2}$ level of the Sm(III) ion was determined to be 2.2 μs from the luminescence decay profile at room temperature by fitting with a monoexponential curve (Fig. S9). For compound **2**, when excited at 395 nm, it exhibits bright red photoluminescence associated with the f–f transitions of $^5D_0$ to ^7F_J (J = 1, 2, 3, 4) at 592, 616, 652 and 699 nm, respectively (Fig. 2c).[19] The intensity ratio of $I(^5D_0 \rightarrow {}^7F_2)/I(^5D_0 \rightarrow {}^7F_1)$ about 3.7 indicates that Eu(III) ions in **2** occupy sites with low symmetry and have no inversion center,[20] which is in accordance with the crystal structure analysis. The observed luminescence decay profile at 616 nm is well fitted with a monoexponential function and yields a lifetime of 0.25 ms (Fig. S10). The total quantum yield Φ is 6.2%. The excitation spectrum of **2** monitored at 616 nm illustrates that a series of f-f absorptions of Eu(III) ion and few ligand absorption, thus proving that the luminescence sensitization through direct excitation of the central Eu(III) ion is much more efficient than the ligand.[21] In order to further support the interaction effects between the organic linker and Lathanide(III) metal sources, the emission spectra of $Sm(NO_3)_3 \cdot 6H_2O$ and $Eu(NO_3)_3 \cdot 6H_2O$ at the same test condition as compounds **1** and **2** have been tested (Fig. S11). As the first excited level of Gd(III) ion is at the high energy level (around 32150 cm^{-1}),[22] the emission spectrum of complex **3** excited at 345 nm displays a broad phosphorescence emission maxima at 545 nm, and a very weak fluorescence emissions centered around 430 nm, resulting from the deprotonated ligand $TPIA^{3-}$ (Fig. 2d). The corresponding lifetimes of these two luminescence peaks are 0.58 ms and 2.39 ns, respectively, with both fitted with a triple-exponential function (Fig. S12). The total quantum yield Φ of **3** is 1.7%. Comparison with the luminescence feature of the ligand in **1** and **3** reveals that the ligand $TPIA^{3-}$ possesses an interesting environment-dependent luminescence emission.

Triplet state of the ligand and energy transfer

It is well-established that the energy match between the energy of ligands and the resonance emission energy level of lanthanide ions is the main factor dominating the luminescence properties of the lanthanide(III) complexes. The lowest excited singlet S1 ($^1\pi\pi^*$) energy of H_3TPIA ligand has been estimated by referring to the wavelength of the UV–vis absorbance edge, which is 30395 cm^{-1} (329 nm) (Fig. S13). The triplet state T1 ($^3\pi\pi^*$) energy can be estimated to be 24272 cm^{-1} (412 nm) corresponding to the lower wavelength emission edge of **3** at 77 K (Fig. S14).[23] According to Reinhoudt's empirical rule,[24] the intersystem crossing (ISC) process

becomes effective when the energy gap ΔE (S1− T1) is at least 5000 cm^{-1}. The ΔE value for the H_3TPIA ligand is 6123 cm^{-1}. Thus, the ISC process is supposed to be efficient. Obviously, the triplet level of H_3TPIA is higher than the resonance energy level of the Sm(III) (17800 cm^{-1}) ion. Therefore, the ligand can effectively transfer energy to the emitting states of the Sm(III) ions[25]. The energy difference between the triplet state of H_3TPIA and the resonance energy level of Eu(III) ion (17300 cm^{-1}) can be calculated to be 6972 cm^{-1}. Latva's empirical rule[26] states that an optimal ligand-to-metal energy transfer process for Eu(III) ions needs [ΔE = E(T1) − E(^5D_J)] 2500–4000 cm^{-1}. Hence, it points out that the energy transfer from ligand to Eu(III) ion is less effective in accordance with the excitation spectra of **2**.

Color-tunable and white-light luminescence

Since the Sm(III) compound **1** provides blue (460 nm), green (562 nm), red (597 and 645 nm) emissions, it is anticipated to achieve white-light emissions by adjusting the blue, green to red intensity ratio. As expected, compound **1** realizes tunable PL behavior from orange to blue through the variation of excitation wavelengths from 340 to 384 nm (Fig. 3). When excited at 340 nm, an orange emission with CIE coordinate of (0.53, 0.36) is obtained. As the excitation wavelength increases, the blue emission intensity from the ligand shows a significant increase, and the emission intensities of green and red components from Sm(III) ion gradually decrease. When the excitation wavelength is 358 nm, the emission intensities from the ligand and Sm(III) ion are comparable, resulting in visible white-light emissions with the CIE coordinate (0.33, 0.31) close to the standard white light (0.33, 0.33) according to 1931 CIE coordinate diagram. The color rendering index (CRI) of 87 and corresponding color temperature (CCT) of 5748 K fall within high-quality white-light source (CCT: 2500 K–6500 K, CRI > 80), as well as a total quantum yield Φ of 1.8%. When increasing the excitation wavelength to 384 nm, the ligand emission dominates the whole emission spectra, which results in a blue emission with the CIE coordinate of (0.26, 0.30). Therefore, the tunable colors from orange to blue are achieved by varying excitation lengths, the corresponding CIE coordinates are recorded in Table S2. Such excitation-dependent photoluminescence tuning in the orange, white and blue regions is presently considered to be controlled by different energy transfer processes[10,11,27]. In the case of higher energy absorption (lower excitation wavelength), the efficient intersystem crossing (ISC) would dominate the whole energy transfer process, which generates orange light of Sm(III) ion emission. In contrast (higher excitation wavelength), when the absorbed energy is too low to allow intersystem crossing to occur, the ligand emission in the blue region dominates. Consequently, a white-light emission can be obtained in **1** by combining the lanthanide(III) ion and ligand luminescence, when an intermediate energy is absorbed.

Considering wide emission band covering from blue to green of **3**, it will therefore be possible to construct white emitting

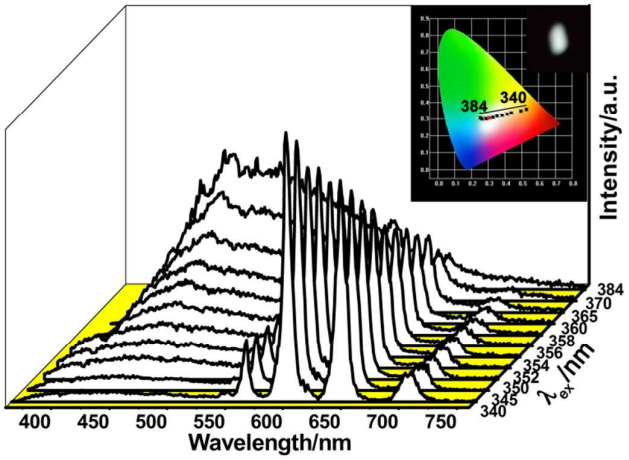

Fig. 3 Emission spectra and 1931 CIE chromaticity diagram (insert) of complex **1** when excited between 340 and 384 nm; inset: optical image of the white light emission in the powdered sample upon excitation at 358 nm.

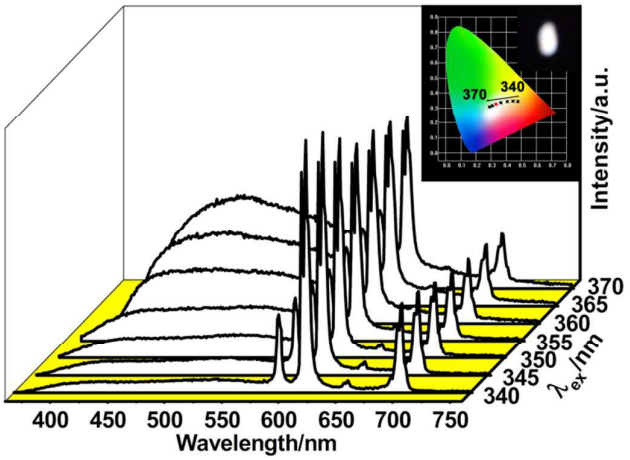

Fig. 4 Emission spectra and 1931 CIE chromaticity diagram (insert) of Eu(III)-doped Gd(III) complex [($Eu_{0.12}Gd_{0.88}$)(TPIA)(H_2O)$_3$]·5.5H_2O **4** when excited between 340 and 370 nm; inset: optical image of the white light emission in the powdered sample upon excitation at 360 nm

materials through doping the red emitting Eu(III) ions into the **3** framework. Following this strategy, we designed and synthesized a mixed-lanthanide(III) CP, [($Eu_{0.12}Gd_{0.88}$)(TPIA)(H_2O)$_3$]·5.5H_2O (**4**), by carefully choosing the starting lanthanide salts. This mixed-lanthanide CP **4** is isomorphous to **1–3** (Fig. S5) and displays not only the characteristic red emissions of the Eu(III) ion at 616 nm, but also the broad blue fluorescence emission of the ligand at 436 nm and green phosphorescence emission at 537 nm upon excited at 340 nm (Fig. S15). Strikingly, it also displays colour tunable and white-light emission character. As the excitation wavelengths increase from 340 to 370 nm, the intensity of blue-green components from the ligand increases, while the red emission intensity of Eu(III) ion slightly decreases (Fig. 4), which reveals that the above-mentioned energy transfer processes are still applicable for **4**. An optimal white emission with the CIE coordinate of (0.33, 0.33), CRI value of 89 and CCT

magnitude of 5489 K, as well as a total quantum yield Φ of 1.9% was attained when excited at 360 nm (Table S3). Furthermore, a series of experiments on different concentrations of Eu(III) ions embedded in the Gd(III) framework **3** were also carried out with the excitation wavelengths turned from 340 to 370 nm. They present the similar variation trend to **4** under different excitation wavelengths (Fig. S16). The CIE coordinates for the Eu(III)-doped Gd(III) complexes are summarized in Table S4.

Conclusions

In summary, single-component Sm(III) and two-component Eu(III)-doped Gd(III) coordination polymers acting as colour tunable and white-light-emitting luminophores have been constructed by a selective light-emitting tetrazolate-dicarboxylate ligand (H_3TPIA), which displays environment-dependent luminescent behaviors. By tailoring the excitation wavelengths, tunable emissions toward white light have been obtained by combining the blue emission of ligand and red-green emission of Sm(III) ion in **1** and blue-green emission of ligand and red emission of Eu(III) ion in **4**. This approach provides a promising platform to achieve color tunable and white-light emitting materials. Our further research will focus on the full-color tunability with a higher quantum yield, and ultimately the fabrication of light-emitting devices.

Acknowledgements

This work was financially supported by 973 Program (2011CBA00505) and National Nature Science Foundation of China (21371170 and 21201099).

Notes and references

1 (a) A. H. Khan, A. Dalui, S. Mukherjee, C. U. Segre, D. D. Sarma, S. Acharya, *Angew. Chem. Int. Ed.,* 2015, **54**, 2643; (b) C.-Y. Sun, X.-L. Wang, X. Zhang, C. Qin, P. Li, Z.-M. Su, D.-X. Zhu, G.-G. Shan, K.-Z. Shao, H. Wu, J. Li, *Nat. Commun.,* 2013, **4**, 2717; (c) I. L. Medintz, H. T. Uyeda, E. R. Goldman, H. Mattoussi, *Nat. Mater.*, 2005, **4**, 435; (d) X. Zhang,; J. Wang, L. Huang, F. Pan, Y. Chen, B. Lei, M. Peng, M. Wu, *ACS Appl. Mater. Interfaces*, 2015, **7**, 10044; (e) W. K. Bae, J. Lim, D. Lee, M. Park, H. Lee, J. Kwak, K. Char, C. Lee, S. Lee, *Adv. Mater.,* 2014, **26**, 6387; (f) M. Shang, C. Li, J. Lin, *Chem. Soc. Rev.*, 2014, **43**, 1372–1386.

2 S. Delikanli, B. Guzelturk, P. L. Hernandez-Martinez, T. Erdem, Y. Kelestemur, M. Olutas, M. Z. Akgul, H. V. Demir, *Adv. Funct. Mater.,* 2015**, 25**, 4282.

3 G. Li, D. Geng, M. Shang, C. Peng, Z. Cheng, J. Lin, *J. Mater. Chem.*, 2011, **21**, 13334.

4 Z. Mao, Z. Yang, Y. Mu, Y. Zhang, Y.-F. Wang, Z. Chi, C.-C. Lo, S. Liu, A. Lien, J. Xu, *Angew. Chem. Int. Ed.,* 2015, **54**, 6270.

5 (a) Y. Cui, Y. Yue, G. Qian, B. Chen, *Chem. Rev.,* 2012, **112**, 1126; (b) Y. Cui, B. Chen, G. Qian, *Coord. Chem. Rev.*, 2014, **273**, 76.

6 (a) Z.-F. Liu, M.-F. Wu, S.-H. Wang, F.-K. Zheng, G.-E Wang, J. Chen, Y. Xiao, A-Q. Wu, G.-C. Guo, J.-S. Huang, *J. Mater. Chem. C*, 2015, **1**, 4634; (b) S. S. Mondal, K. Behrens, P. R. Matthes, F. Schoenfeld, J. Nitsch, A. Steffen, P.-A. Primus, M. U. Kumke, K. Mueller-Buschbaum, H.-J. Holdt, *J. Mater. Chem. C*, 2015, **3**, 4623.

7 Y. Cui, T. Song, J. Yu, Y. Yang, Z. Wang, G. Qian, *Adv. Funct. Mater.,* 2015, **25**, 4796.

8 A. R. Ramya, S. Varughese, M. L. P. Reddy, *Dalton Trans.*, 2014, **43**, 10940.

9 (a) D. F. Sava, L. E. S. Rohwer, M. A. Rodriguez, T. M. Nenoff, *J. Am. Chem. Soc.*, 2012, **134**, 3983; (b) Y.-H. Zhang, X. Li , S. Song, *Chem. Commun.,* 2013, **49**, 10397; (c) S. Song, X. Li, Y.-H. Zhang, *Dalton Trans.*, 2013, **42**, 10409.

10 (a) S.-M. Li, X.-J. Zheng, D.-Q. Yuan, A. Ablet, L.-P. Jin, *Inorg. Chem.*, 2012, **51**, 1201; (b) C. Feng, J.-W. Sun, P.-F. Yan, Y.-X. Li, T.-Q. Liu, Q.-Y. Sun, G.-M. Li, *Dalton Trans.*, 2015, **44**, 4640

11 Q.-Y. Yang, K. Wu, J.-J. Jiang, C.-W. Hsu, M. Pan, J.-M. Lehn, C.-Y. Su, *Chem. Commun.*, 2014, **50**, 7702.

12 (a) K. Binnemans, *Chem. Rev.*, 2009, **109**, 4283; (b) M. D. Allendorf, C. A. Bauer, R. K. Bhakta, R. J. T. Houk, *Chem. Soc. Rev.*, 2009, **38**, 1330.

13 (a) M. Giraud, E. S. Andreiadis, A. S. Fisyuk, R. Demadrille, J. Pécaut, D. Imbert, M. Mazzanti, *Inorg. Chem.*, 2008, **47**, 3952; (b) E. S. Andreiadis, D. Imbert, J. Pecaut, R. Demadrille, M. Mazzanti, *Dalton Trans.*, 2012, **41**, 1268; (c) N. M. Shavaleev, S. V. Eliseeva, R. Scopelliti, J.-C. G. Bünzli, *Inorg. Chem.*, 2014, **53**, 5171; (d) J. Jia, J. Xu, S. Wang, P. Wang, L. Gao, M. Yu, Y. Fan, L. Wang, *CrystEngComm*, 2015, **17**, 6030.

14 (a) J. Chen, Q. Zhang, Z.-F. Liu, S.-H. Wang, Y. Xiao, R. Li, J.-G. Xu, Y.-P. Zhao, F.-K. Zheng, G.-C. Guo, *Dalton Trans.*, 2015, **44**, 10089; (b) S.-H. Wang, F.-K. Zheng, M.-J. Zhang, Z.-F. Liu, J. Chen, Y. Xiao, A-Q. Wu, G.-C. Guo, J.-S. Huang, *Inorg. Chem.*, 2013, **52**, 10096; (c) F. Chen, M.-F. Wu, G.-N. Liu, M.-S. Wang, F.-K. Zheng, C. Yang, Z.-N. Xu, Z.-F. Liu, G.-C. Guo, J.-S. Huang, *Eur. J. Inorg. Chem.*, 2010, 4982.

15 P. Lama, A. Aijaz, E. C. Sanudo, P. K. Bharadwaj, *Cryst. Growth Des.*, 2010, **10**, 283.

16 CrystalClear, version 1.35, *Software User's Guide for the Rigaku R–Axis, and Mercury and Jupiter CCD Automated X–ray Imaging System*, Rigaku Molecular Structure Corporation, Utah, 2002.

17 *SHELXTL Reference Manual*, *version 5*, Siemens Energy & Automation Inc., Madison, WI, 1994.

18 (a) H. He, F. Sun, H. Su, J. Jia, Q. Li, G. Zhu, *CrystEngComm*, 2014, **16**, 339; (b) D. Li, J. Y. Sun, L. Wang, L. Y. Zhang, X. H. Liu, J. N. Xu, P. Zhang, *Inorg. Chim. Acta*, 2013, **399**, 154.

19 S. V. Eliseeva, J.-C. G. Buenzli, *Chem. Soc. Rev.*, 2010, **39**, 189.

20 A. F. Kirby, D. Foster, F. S. Richardson, *Chem. Phys. Lett.*, 1983, **95**, 507.

21 (a) S. Biju, D. B. A. Raj, M. L. P. Reddy, B. M. Kariuki, *Inorg. Chem.*, 2006, **45**, 10651; (b) C. Gao, A. M. Kirillov, W. Dou, X. Tang, L. Liu, X. Yan, Y. Xie, P. Zang, W. Liu, Y. Tang, *Inorg. Chem.*, 2014, **53**, 935.

22 (a) Y. Cui, Y. Yue, G. Qian, B. Chen, *Chem. Rev.*, 2012, **112**, 1126; (b) L. Armelao, S. Quici, F. Barigelletti, G. Accorsi, G. Bottaro, M. Cavazzini, E. Tondello, *Coord. Chem. Rev.,* 2010, **254,** 487.

23 (a) P. N. Remya, S. Biju, M. L. P. Reddy, A. H. Cowley, M. Findlater, *Inorg. Chem.*, 2008, **47**, 7396; (b) X. Zhou, X. Zhao, Y. Wang, B. Wu, J. Shen, L. Li, Q. Li, *Inorg. Chem.,* 2014, **53**, 12275.

24 F. J. Steemers, W. Verboom, D. N. Reinhoudt, E. B. Vander Tol, J. W. Verhoeven, *J. Am. Chem. Soc.*, 1995, **117**, 9408.

25 G. A. Crosby, R. E. Whan, R. M. Alire, *J. Chem. Phys.,* 1961, **34**, 743.

26 M. Latva, H. Takalo, V. M. Mukkala, C. Matachescu, J. C. Rodríguez-Ubisd, J. Kanakare, *J. Lumin.*, 1997, **75**, 149.

27 (a) B.-B. Du, Y.-X. Zhu, M. Pan, M.-Q. Yue, Y.-J. Hou, K. Wu, L.-Y. Zhang, L. Chen, S.-Y. Yin, Y.-N. Fan, C.-Y. Su, *Chem. Commun.*, 2015, **51**, 12533; (b) F. Zhang, P. Yan, H. Li, X. Zou, G. Hou, G. Li, *Dalton Trans.*, 2014, **43**, 12574.

Graphical Abstract

Excitation wavelength-induced color tunable and white-light emissions in lanthanide(III) coordination polymers constructed by an environment-dependent luminescent tetrazolate-dicarboxylate ligand

Yu Xiao,[a,b] *Shuai-Hua Wang,*[a] *Fa-Kun Zheng,*[*,a] *Mei-Feng Wu,*[c] *Ju-Xu,*[a] *Zhi-Fa Liu,*[a] *Jun Chen,*[a,b] *Rong Li*[a,b] *and Guo-Cong Guo*[a]

[a] *State Key Laboratory of Structural Chemistry, Fujian Institute of Research on the Structure of Matter, Chinese Academy of Sciences, Fuzhou, Fujian 350002, P. R. China*

[b] *University of Chinese Academy of Sciences, Beijing 100039, P. R. China*

[c] *School of Environmental and Chemical Engineering, Nanchang Hangkong University, Nanchang, Jiangxi 330063, P. R. China*

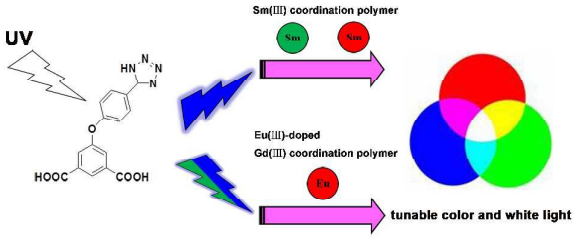

Single-component Sm(III) and two-component Eu(III)-doped Gd(III) coordination polymers acting as color tunable and white-light emitting luminophores have been constructed by a selective light-emitting tetrazolate-dicarboxylate ligand.